

3D Shape Segmentation via Shape Fully Convolutional Networks

Pengyu Wang^{1,2} Yuan Gan^{1,2} Yan Zhang^{1,2} Panpan Shui^{1,2}

¹State Key Lab for Novel Software Technology, Nanjing University, China

²Department of Computer Science and Technology, Nanjing University, China

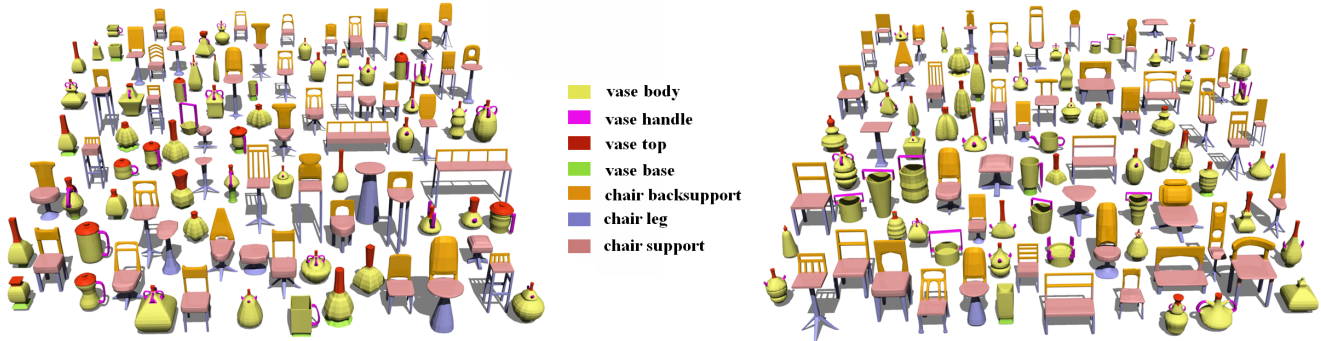


Figure 1: Example of our shape segmentation results on one mixed shape dataset. The shapes on the left are part of training set, and some segmentation results are shown on the right.

Abstract

We propose a novel fully convolutional networks architecture for shapes, denoted as *Shape Fully Convolutional Networks (SFCN)*. Similar to convolution and pooling operation on image, the 3D shape is represented as a graph structure in the SFCN architecture, based on which we first propose and implement *shape convolution and pooling operation*. Meanwhile, to build our SFCN architecture in the original image segmentation FCN architecture, we also design and implement the *generating operation* with bridging function. This ensures that the convolution and pooling operation we designed can be successfully applied in the original FCN architecture. In this paper, we also present a new shape segmentation based on SFCN. In contrast to existing state-of-the-art shape segmentation methods that require the same types of shapes as input, we allow the more general and challenging input such as *mixed datasets of different types of shapes*. In our approach, SFCNs are first trained end-to-end, triangles-to-triangles by three low-level geometric features. Then, based on the trained SFCNs, we can complete the shape segmentation task with high quality. Finally, The feature voting-based multilabel graph cuts is adopted to optimize the segmentation results obtained by SFCN prediction. The experiment results show that our method can effectively learn and predict mixed shape datasets of either similar or different characters, and achieve excellent segmentation results.

1 Introduction

Shape segmentation aims to divide the 3D shape into meaningful parts and to reveal its internal structure, which is the basis and prerequisite to explore the inherent law of the shape. The results obtained from shape segmentation can be applied to various fields of computer graphics, such as shape editing [Yu et al. 2004], deformation [Yang et al. 2013], and modeling [Chen et al. 2015]. Shape segmentation, therefore, has become one of the research hotspots yet difficulties in the fields of digital geometric model processing and instance modeling.

Convolutional networks have shown excellent performance in various image processing problems such as image classification [Krizhevsky et al. 2012; Szegedy et al. 2015; Simonyan and Zisserman 2014], and semantic segmentation [Ciresan et al. 2012; Farabet et al. 2013; Pinheiro and Collobert 2013]. With the emerging encouraging study results, many researchers have been devoted to various deformation studies on CNNs, one of which is fully convolutional network (FCN) [Long et al. 2015]. This method can train end-to-end, pixels-to-pixels on semantic segmentation, with no requirement on the size of the input image. Thus, it has become one of the key research topics in CNN networks.

Although FCN can generate good results in image segmentation, we cannot directly apply it to 3D shape segmentation. This is mainly because image is a kind of a static 2D array, which has a very standard data structure and regular neighborhood relations. Therefore, convolution and pooling can be easily operated when processing FCN. While the data structure of 3D shape is irregular, which cannot be directly represented as the data structure of image. As triangle meshes have no regular neighborhood relations like image pixels, direct convolution and pooling operation on 3D shape is difficult to fulfill. Accordingly, FCN cannot be immediately implemented to complete segmentation.

Inspired by the FCN architecture in image segmentation, we design and implement a new FCN architecture that operates directly on 3D shapes. We firstly represent a 3D shape as a graph structure. Based on the FCN process of convolution and pooling operation on the image and existing methods of Graph Convolutional Neural Networks [Edwards and Xie 2016; Niepert et al. 2016; Defferrard et al. 2016], we propose shape convolution and pooling operation, which can be applied directly on the 3D shape. Combined with the original FCN architecture, we build a new shape fully convolutional network architecture and name it *Shape Fully Convolutional Networks (SFCN)*. Secondly, following the SFCN architecture mentioned above and the basic flow of image segmentation of FCN [Long et al. 2015], we devise a novel trained end-to-end, triangles-to-triangles model for shape segmentation. Thirdly, for higher accuracy of segmentation, we use the multiple features of the shape to complete the training on the SFCN. Utilizing the com-

plementarity between features and combined with multilabel graph cuts method [Boykov et al. 2001; Kolmogorov and Zabih 2004; Boykov and Kolmogorov 2004], we optimize the segmentation results obtained by SFCN prediction, through which the final shape segmentation results are obtained. Our approach can realize the triangles-to-triangles leaning and prediction with no requirements on the triangle numbers of the input shape. Furthermore, many experiments show that our segmentation results perform better than that of the existing methods [Kalogerakis et al. 2010; Guo et al. 2015; Xie et al. 2014], especially when dealing with large dataset. Last but not the least, the proposed method permits mixed dataset learning and prediction. Datasets of different types are combined together in the test, and the accuracy of the segmentation results of different shapes decreased very little. As shown in Figure 1, for a mixed shape dataset from COSEG [Wang et al. 2012] with several types of shapes, part of the training set are displayed on the left, and some corresponding segmentation results are shown on the right. Figure 2 shows the process of our method.

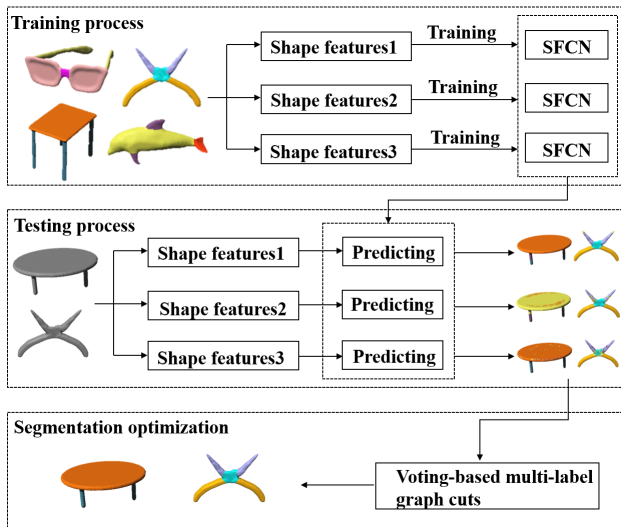


Figure 2: The pipeline of our method. It may divide into 3 stages: training process, using the proposed SFCN architecture to train under three different features; testing process, predicting the test sets through the SFCN architecture; optimization process, optimizing the segmentation results by the voting-based multilabel graph cuts method to get the final segmentation results.

The main contributions of this paper including :

1. To the best of our knowledge, the shape fully convolutional network architecture, named as Shape Fully Convolutional Networks (SFCN) is proposed for the first time, which is able to achieve the convolution and pooling operation on the 3D shape.
2. We present a novel shape segmentation based on SFCN. It can train end-to-end, triangles-to-triangles by three low-level geometric features and outperforms the state-of-the-arts in shape segmentation.
3. More importantly, our method can also be applied to train and predict mixed datasets of different types of shapes.

2 Related Work

Fully convolutional networks. The fully convolutional networks [Long et al. 2015] proposed in 2015 is a pioneering research, which can effectively solve the problem of semantic image segmentation

by pixel level classification. Later, a great deal of research has emerged based on the FCN algorithms and achieved good results in various fields such as edge detection [Xie and Tu 2015], depth regression [Liu et al. 2015], optical flow [Dosovitskiy et al. 2015], simplify sketch [Simo-Serra et al. 2016] and so on. However, the existing research on FCN is mainly restricted to image processing, largely because image has a standard data structure, easy for convolution, pooling and other operation. As shape data used in this paper does not have a standard data structure, it is difficult to directly use the original FCN architecture for computing. In our work, we design convolution and pooling operation suitable for shape data structure based on its features. Besides, inspired by the original FCN architecture, we implement our own shape fully convolutional networks.

Supervised methods for segmentation and labeling. When using the supervised method to train a collection of labeled 3D shapes, advanced machine learning approach is used to complete the related training [Kalogerakis et al. 2010; Guo et al. 2015; Xie et al. 2014; Wang et al. 2012; Wang et al. 2013]. The learning architecture obtained from training is then used to predict other untrained shapes. For example, Kalogerakis et al. used Conditional Random Fields (CRF) to model and learn the sample example, so as to realize the component segmentation and labeling of 3D mesh shape. Wang et al. first projected 3D shapes to 2D space and the labeling results in 2D space were then projected back to 3D shapes for mesh labeling. Xie et al. [2014] use Extreme Learning Machine (ELM), which can be used for consistency segmentation for unknown shapes, to realize shape segmentation. Guo et al. [2015] applied Convolutional Networks Neural (CNN) to complete the shape segmentation. All of these approaches have achieved impressive segmentation results. Our's also belongs to them. We use the SFCN architecture to complete the shape segmentation, which can automatically train end-to-end, triangles-to-triangles and output high quality segmentation results. Moreover, our method is more suitable to deal with large datasets, as with the increase of datasets, the learning ability of our method gradually becomes stronger. This method is also applicable to learn and predict mixed datasets.

Unsupervised segmentation and labeling. A lot of research methods can build segmentation model [Huang et al. 2011; Sidi et al. 2011; Hu et al. 2012; Meng et al. 2013; Xu et al. 2010] and achieve joint segmentation by the direct analysis of the correlation of the same shape, without any label information. There are mainly two unlabeled methods: matching and clustering. Using matching method, the matching relation between pair 3D shapes is obtained based on the similarity of relative unit given by correlation calculation. The segmentation shape of matching shape is then established to realize the joint segmentation [Kreavoy et al. 2007; Huang et al. 2011] of 3D shapes. By contrast, clustering methods analyze all the 3D shapes in the model set, cluster the consistent correlation units of 3D shapes into the same class. Then a segmentation model is obtained and applied to consistent segmentation [Hu et al. 2012; Meng et al. 2013; Xu et al. 2010]. To obtain accurate segmentation results, these unsupervised shape segmentation methods must be trained on the same type of shapes. However, our SFCN method has a strong generalization ability, thus it can complete the mixed dataset training and learning, and realize the segmentation of mixed datasets.

3 Shape Fully Convolution Network

In the process of image semantic segmentation, it is mainly through operation such as convolution and pooling that fully convolution network architecture complete the image segmentation [Long et al. 2015]. As analyzed above, the regular data structure

among the pixels of the image makes it is easy to implement these operation. In analogy with image, triangles of the 3D shape can be seen as pixels on the image, but unlike pixels, triangles of the shape have no ordered sequence rules. Figure 3(a) represents the regular pixels on the image, while Figure 3(b) represents the irregular triangles on the shape. As can be seen, the two arrangements are completely different. It is difficult to complete the convolution and pooling operation on the 3D shape like that of the image. Therefore, based on the characteristics of 3D shape data structure and analogous to the operation on the image, we need to design new shape convolution and pooling operation.

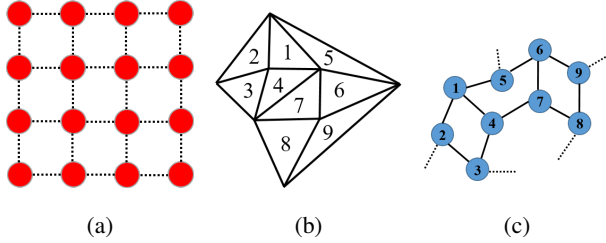


Figure 3: Representation of different forms of data. (a) Image data representation; (b) Shape data representation; (c) Shape data represented as graph structure.

As 3D shape is mainly composed of triangles and connections among them, we can use graph structure to describe it. Each 3D shape can be represented as $G = (V, E)$, with vertex $v \in V$ for triangle and edge $e \in E \subset V \times V$ for the connection of adjacent triangles. The small triangle shown in 3(b) corresponds to the graph structure shown in Figure 3(c). Based on the graph structure, we design and implement *shape convolution and pooling operation*, which will be detailed in the following part.

3.1 Convolution on Shape

Convolution is one of the two key operations in the FCN architecture, allowing for locally receptive features to be highlighted in the input image. When convolution is applied to images, a receptive field (a square grid) moves over each image with a particular step size. The receptive field reads the pixels feature values, for each channel once, and a patch of values is created for each channel. Since the pixels of an image have an implicit arrangement, a spatial order, the receptive fields always move from left to right and top to bottom. Analogous to the convolution operation on the image, therefore, we need to focus on the following two key emphases when employing convolution operation on the shapes:

1. Determining the neighborhood sets around each triangle for convolution operation according to the size of the receptive field.
2. Determining the order of execution of convolution operation on each neighborhood set.

For the first emphasis, the convolution operation on the image is mainly based on the neighborhood relationship between pixels. Accordingly, we need to construct locally connected neighborhoods from the input shape. These neighborhoods are generated efficiently and serve as the receptive fields of a convolutional architecture, permitting the architecture to learn shape representations effectively.

Shape has neighborhood relationship just like image, but its irregularity restrains it to be directly represented and applied to the FCN learning. Yet when it is expressed as graph structures, the locally connected neighborhoods of each triangle of the shape can be eas-

ily determined with various search strategies. In this paper, each triangle of the shape is viewed as the source node. We use the breadth-first search to expand its neighborhood nodes on the constructed graph so as to obtain the neighborhood sets of each triangle in the shape. Suppose the receptive field is set as K , the size of the neighborhood set will be the same as it, including $K - 1$ neighborhood nodes and a source node, all of which will be used for follow-up convolution operation. Figure 4(a) shows the graph structure of the shape, while Figure 4(b) shows the neighborhood sets of each source node (that is, each triangle on the 3D shape) we obtained with the method mentioned above.

As for the second emphasis, when performing the convolution operation on the image, it is easy to determine the order of convolution operation according to the spatial arrangement of the pixels. However, it is rather difficult to determine the spatial orders among triangles on the 3D shape. A new strategy is thus needed to reasonably sort the elements in the neighborhood sets. Sorting is to ensure that the elements in each neighborhood set can be convolved by the same rules, so that the convolution operation can better activate features. For each node, all nodes in its neighborhood set can be sorted by the feature distance. By this way, we can not only determine the order of convolution operation of each neighborhood set, but also ensure that the nodes in different sets have the same contribution regularity to their own source nodes in convolution operation. The final convolution order for each neighborhood set is shown in Figure 4(c). As shown in Figure 4(b), the execution order of convolution operation of the neighborhood set obtained from the source node, is determined by calculated feature distance.

3.2 Pooling on Shape

Pooling is the other key operation in the FCN architecture. The pooling operation is utilized to compress the resolution of each feature map (the result of convolution operation) in the spatial dimensions, leaving the number of feature maps unchanged. Applying a pooling operation across a feature map enables the algorithm to handle a growing number of feature maps and generalizes the feature maps by resolution reduction. Common pooling operation are that of taking the average and max of receptive fields over the input map [Edwards and Xie 2016]. We share the same pooling operation on shape fully convolutional network with operation mentioned above. However, we need to address a key concern, that is, to determine the pooling operating order of the SFCN on the shape feature map.

Similar to convolution operation, we cannot directly determine the pooling operation order on SFCN based on spatial relationships among the triangles of the 3D shape. Since the 3D shape has been expressed as graph structure, we can determine the pooling operation order according to the operation of convolutional neural networks on graph. In this paper, the pooling operation on SFCN is computed by adopting the fast pooling of graph [Niepert et al. 2016; Defferrard et al. 2016].

The pooling method for graph [Niepert et al. 2016; Defferrard et al. 2016] coarsens graph with Graclus multilevel clustering algorithm [Dhillon et al. 2007]. Graph coarsening aims to determine the new structure of the graph after pooling. We first present each shape as graph structure, then we exploit the feature information on the triangles of the shape and Graclus multilevel clustering algorithm [Dhillon et al. 2007] to complete shape coarsening, that is, to determine the new connection relationship of the shape feature map after pooling, which is shown in Figure 5(a).

In the pooling process, traversing feature map in certain order according to the size of the receptive field is a key step to complete

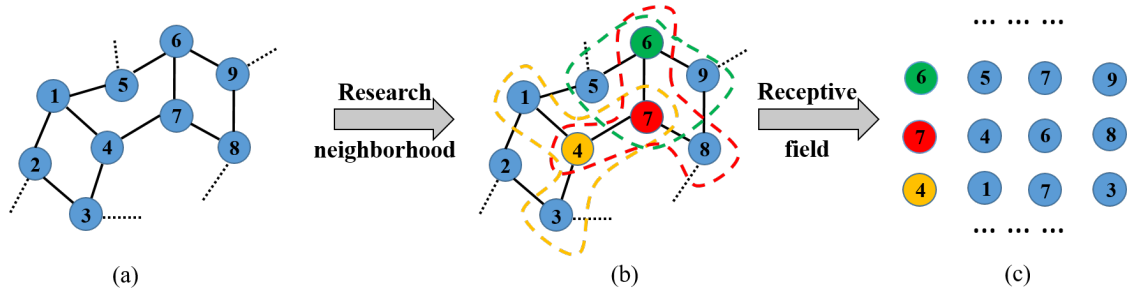


Figure 4: Convolution process on shape. (a) Shape represented as graph; (b) The neighborhood nodes of different source nodes searched by breadth-first search, among which 4, 6, 7 represent source nodes. The areas circled by orange, red and green dotted line are the neighborhood nodes searched by each source node. (c) Convolution order of each neighborhood set. The ellipsis is for other neighborhood sets not represented.

the calculation, namely, to determine the operation order of pooling. Following the method of pooling for graph proposed by [Deferrard et al. 2016], the vertices of the input graph and its coarsened versions are irregularly arranged after graph coarsening. To define the pooling order, therefore, a balanced binary tree is built by adding fake code to sort the vertices. Lastly, the pooling operation of graph is completed based on the nodes order and the use of 1D signal pooling method. After shape coarsening, we apply the same approach in this study to determine the order of pooling operation on shape fully convolutional networks architecture, as shown in Figure 5(b).

4 Shape Segmentation via Shape Fully Convolution Network

We design a novel shape segmentation method based on SFCN, analogous to the basic process of image semantic segmentation on FCN [Long et al. 2015]. Firstly, we extract three types of commonly used geometric features of the shape as an input for SFCN training and learning. Secondly, based on the shape convolution and pooling operation proposed in Section 3 and the basic process of image semantic segmentation on FCN, we designed a lattice structure suitable for 3D shape segmentation. Through training and learning of the network, we can complete end-to-end, triangles-to-triangles prediction. Finally, we introduce the optimization process of shape segmentation.

4.1 Geometric Feature Extraction

Our approach is designed to complete the network training and learning based on some common and effective low-level features. In this paper, therefore, we extract three from the existing commonly used ones as the main features for the network training and learning. The three types of features include: average geodesic distance (AGD) [Hilaga et al. 2001], shape context (SC) [Belongie et al. 2002] and spin image (SI) [Johnson and Hebert 1999]. These features can well describe the characteristics of each triangle on a shape from multiple perspectives. We also found in the experiment that these three features are complementary, which will be analyzed in detail in the experimental part.

4.2 Shape Segmentation Networks Structure

As the convolution and pooling operation on shape are different from that on image, the FCN architecture originally used in image segmentation cannot be directly applied on the 3D shape. We

modify the original FCN architecture according to the convolution and pooling characteristics, so that it can be conducted in shape segmentation.

Our training network is made up of four parts: *convolution, pooling, generating and deconvolution layer*, as shown in Figure 6. The convolution layer corresponds to feature extractor that transforms the input shape to multidimensional feature representation. The convolution operation is completed by the method proposed in section 3.1. The pooling layer is used to reduce feature vector of the convolution layer, and expand its receptive field to integrate feature points in the small neighborhood into the new ones as output. The pooling operation is completed by the method proposed in section 3.2.

As our convolution and pooling operation are designed for shape, the original FCN architecture cannot be used directly. Through the above analysis we know, compared with the original FCN's architecture, the SFCN's in this paper needs to record every neighborhood set of each shape participated in convolution obtained in Section 3, as well as the convolution and pooling order of each shape. Thus, we add a *generating layer* in the original FCN architecture, whose diagram of concrete meaning is shown in Figure 7. Firstly, as shown in Figure 7(a), we can calculate the pooling order between nodes of the graph by shape pooling method proposed in Section 3.2, (these nodes are equivalent to the triangle of the shape). We store the nodes in the calculation order on the *generating layer*, as shown in Figure 7(c). Figure 7(a) gives the pooling order on a shape, where the figures represent the number of nodes (i.e. triangles). Secondly, we need to record the neighborhood sets of each node (i.e. each triangle of the shape) involved in convolution computation, as shown in Figure 7(b), where we store the neighborhood sets by reading the offset in Figure 7(a). After the nodes are sorted by column on the *generating layer*, we record their neighborhood sets, in which the nodes are sorted according to the convolution order calculated in Section 3.1. As shown in Figure 7(c), each row which are sequenced in the convolution order represents a neighborhood set of a node, where the figures represent the number of nodes (i.e. triangle). By storing the data in this way, we can achieve the convolution operation by row and the pooling operation by column, as shown in Figure 7(c). Another advantage of such storage is that, after pooling, the new neighborhood set and the pooling order required by the next convolution layer of each new node can still be obtained and be applied to the next *generating layer* with the method in Section 3.2. In this paper, we add a *generating layer* to each convolution layer, to ensure the correct order of the subsequent convolution and pooling calculation. In other words, the order of each shape is predetermined with the method in Section 3 before the training. Then they are provided

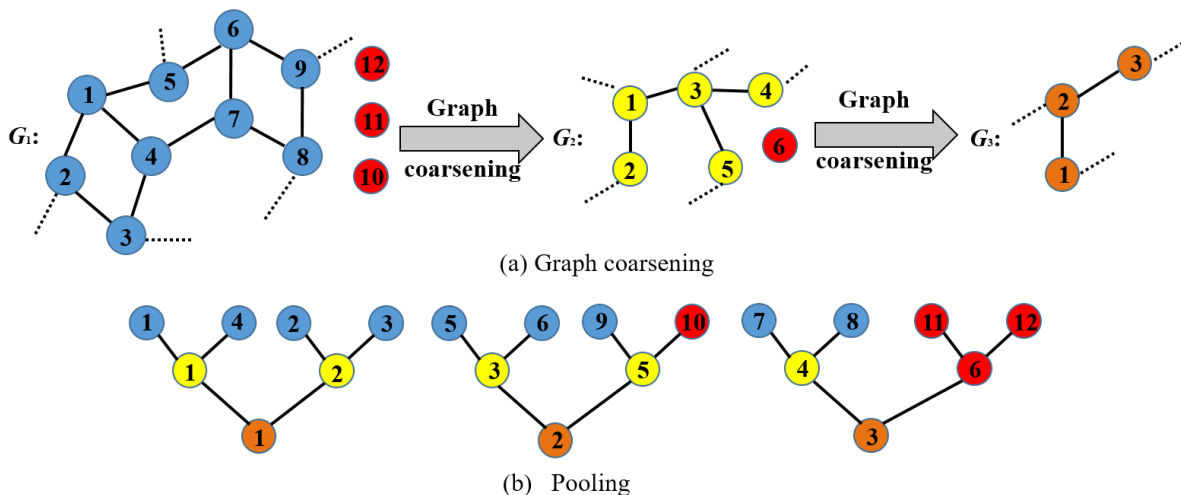


Figure 5: Example of graph coarsening and pooling. (a) Graph coarsening process. Note: original graph has 9 arbitrarily ordered vertices. For a pooling of size 4, two coarsenings of size 2 are needed. To ensure that in the coarsening process the balanced binary tree can be constructed, we need to add appropriate fake nodes through calculation, which are identified in red. After coarsening, the node order on G_3 is still arbitrary, yet it can be manually set. Then backstepping the coarsening process, we can determine the node order of G_2 and G_1 , and the corresponding relationship between nodes in each layer according to the order of G_3 . At that point the arrangement of vertices in G_1 permits a regular 1D pooling. (b) Pooling order. The nodes in first layer (blue and red) represent the G_1 node order; the second layer (yellow and red) represent G_2 node order; the third layer (purple) represent the G_3 node order and the corresponding relationship between nodes in each layer. The red nodes are fake nodes, which is set to 0 in the pooling process, as we carry out max pooling.

to the *generating layer*, served as bridge, so that subsequent calculations can be carried out. Deconvolution layer is a shape generator that produces shape segmentation from the feature extracted from the convolution layer. In this paper, the width of convolution kernel in the deconvolution layer of the original FCN architecture is changed to 1 and the height is set to the size of the pooling we use, thereby getting the deconvolution layer of SFCN. The final output of layer is a probability map, indicating probability of each triangle on a shape that belongs to one of the predefined classes.

Based on the FCN architecture proposed by Long et al., we design a SFCN architecture suitable for shape segmentation. Our convolution has five convolutional layers altogether, with each convolution layer having a generating layer before generating data for the next convolution and pooling and followed by a pooling layer. Two fully connected layers are augment at the end to impose class-specific projection. Corresponding to the pooling layer, there are five deconvolution layers, through which we can obtain the prediction probability of each triangle of the shape that belongs to each class, as shown is Figure 6. In the prediction process, we used the same skip architecture [Long et al. 2015]. It can combine segmentation information from a deep, coarse layer with appearance information from a shallow, fine layer to produce accurate and detailed segmentations as the original FCN architecture. The specific process is shown in Figure 8. The prediction probability of each layer can be obtained by adding the results of deconvolution layer and the corresponding results of the pooling layer after convolution, which also functions as the input of the next deconvolution layer. The number of rows will be repeated 5 times to return to the initial number of triangles, where the value of each channel is the probability of this class, realizing the triangle level prediction. Another difference from the original FCN architecture is that, to normalize the data, we add a batch normalization layer after the convolution operation of the first layer of the original FCN architecture, using the default implementation of the BN in the Caffe [Jia et al. 2014].

4.3 Shape Segmentation Optimization

Because the feature dimensions we use and what these features represent are different, we will train these features separately using the network structure provided in Section 4.2. Given the testing shape, we can get the corresponding segmentation results under each feature, which can describe the segmentation of 3D shapes from different perspectives. Besides, due to the different starting points of the features, there may be some differences among the predicted segmentation results of the same shape. To obtain the final segmentation results, we leverage the complementarity among features and the multilabel graph cuts method [Boykov et al. 2001; Kolmogorov and Zabih 2004; Boykov and Kolmogorov 2004] to optimize the segmentation results of the testing shape. The final segmentation result is obtained mainly through the optimization of the following formula.

$$E(l) = \sum_{u \in V} E_D(u, l_u) + \sum_{\{u, v\} \in E} E_S(u, v, l_u, l_v). \quad (1)$$

In this formula, l_u and l_v are labels of triangle u and v , data item $E_D(u, l_u)$ describes the energy consumption of triangle u marked as label l_u , and smoothing item E_S describes the energy consumption of neighboring triangles marked as different labels.

The first item of the formula is optimized mainly based on the probability that triangle u is marked as label l_u . We predict the shape under the three features respectively, so the same triangle u will have their own prediction probability under each feature. In this paper, utilizing the feature’s complementarity, we vote the labeling results to get the final prediction probability, and serve its negative logarithm similar to the paper [Guo et al. 2015] as the first item of the multilabel graph cut. The second item in the formula smooths the segmentation results mainly through the calculation of the dihedral angle of the triangle and its neighboring one. In this paper, the dihedral angle multiplied by the side length makes the second item of the formula to complete optimization. Energy

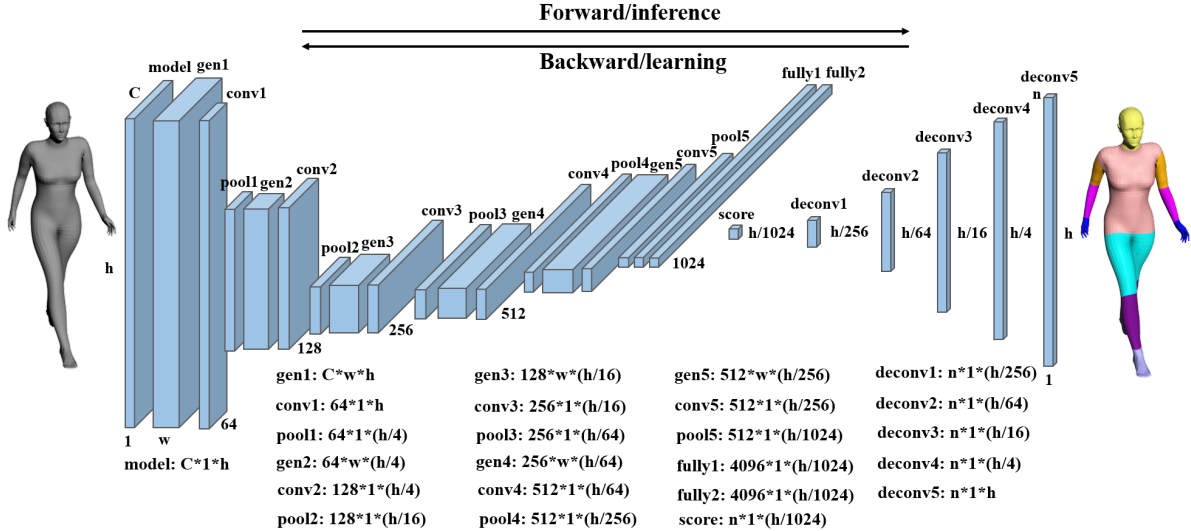


Figure 6: The SFCN architecture we designed, mainly including 4 parts: convolution, pooling, generating, and deconvolution layer, which are represented as gen, con, pool and deconv respectively. Besides, fully is for fully connectivity and the numerical values reflect the dimension changes of each layer after calculation. C represents feature dimension, h represents the number of triangles of each shape and n represents the shape segmentation labels.

E is minimized by employing Multilabel Graph Cuts Optimization [Boykov et al. 2001; Kolmogorov and Zabih 2004; Boykov and Kolmogorov 2004], through which we can obtain more accurate shape segmentation results.

5 Experimental Results and Discussion

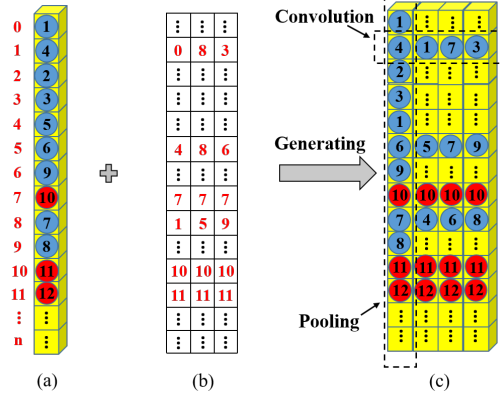


Figure 7: Diagram of generating layer. (a) The pooling order: Red number stands for the offset, nodes in the blue circles represents nodes on the graph, nodes in the red circles are fake nodes. (b) Recorded neighborhood set of each node. The numbers in the table represent the offset of each node after pooling sorting. (c) Data storage of the generating layer proposed in this paper, based on which our method can implement convolution operation by row and pooling operation by column.

Data. In this paper, deep learning is used to segment the shape, therefore to verify the effectiveness of this method, we first test 3 existing large datasets from COSEG [Wang et al. 2012], including the chair dataset of 400 shapes, the vase dataset of 300 shapes and the alien dataset of 200 shapes. The experiment of the mixed dataset is carried out as well on the Princeton Segmentation Bench-

mark (PSB) [Chen et al. 2009] dataset. In addition, to confirm the robustness of the above method, we also select 11 categories in the PSB [Chen et al. 2009] dataset for testing, each of them containing 20 shapes. For COSEG datasets, we choose the groundtruth as in the paper [Wang et al. 2012]. For PSB datasets, we choose the groundtruth as in the dissertation [Kalogerakis et al. 2010].

SFCN Parameters. We train by SGD with momentum, using momentum 0.9 or 0.99 and weight decay of $1e-4$ or $1e-2$. We choose ReLU as activation function. Dropout used in the original classifier nets is included. The per-triangle, unnormalized softmax loss is a natural choice for segmenting shapes of any size, with which we train our nets.

Computation Time. We use two Intel(R) Xeon(R) CPU E5-2620 v3 @ 2.40GHz with 12 cores and NVIDIA GeForce TITAN X GPU. In large datasets, when we use 50 shapes for training and the triangles of each shape range from 1000 to 5000, the training would take about 40 minutes and the test and optimization of a shape take about 30 seconds.

Results. In the experiment, we used the classification accuracy proposed by Kalogerakis [Kalogerakis et al. 2010] and Sidi [Sidi et al. 2011] for the quantitative evaluation of our method.

Firstly, to compare with the methods of [Guo et al. 2015] in the COSEG's large dataset, we randomly selected 50 shapes for training in the chair dataset and 20 shapes for training in the vase dataset. We compare our method with three shape segmentation methods [Sidi et al. 2011; Kim et al. 2013; Guo et al. 2015]. The results are represented in Table 1. It should be noted that the results and data obtained by other methods come from [Guo et al. 2015]. The table shows that the results obtained by the proposed method outperform these existing methods, and it is proved that our method is effective.

Secondly, to verify the effectiveness of the proposed method in large dataset, we randomly select 25%, 50% and 75% shapes for training from each three large datasets of COSEG. To verify whether the SFCN prediction accuracy becomes higher as the number of training sets increases, we use the same 25% shapes for

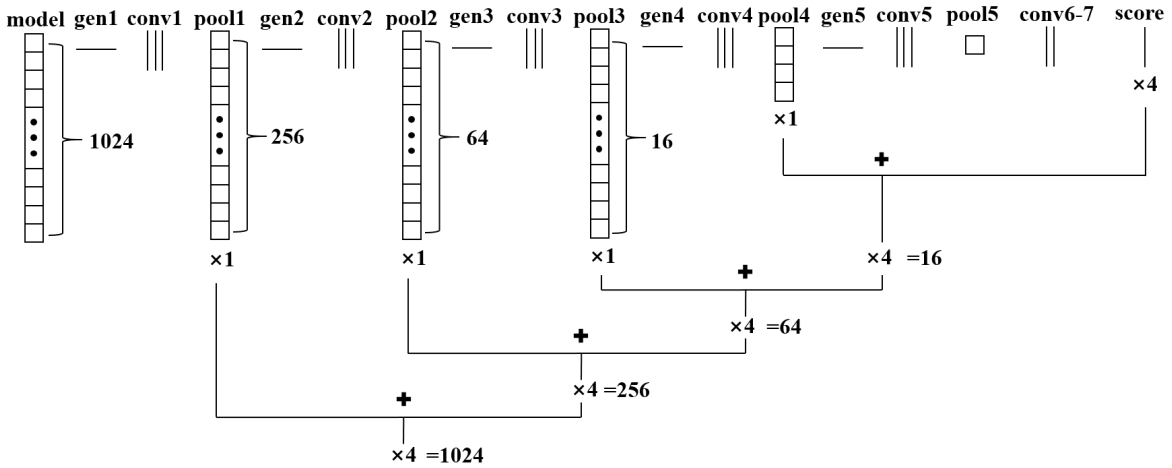


Figure 8: The skip architecture for prediction. Our DAG nets learn to combine the coarse, high layer information with the fine, low layer one. We get the prediction results of the final layer by upsampling the score, then upsample again the prediction results combined the final layer and the pool4 layer. After 5 times upsampling, we obtain the final prediction results, combined the final layer, pool5, pool4, pool3, pool2 and pool1 layer information, which can achieve triangles-to-triangles prediction.

Table 1: Labeling Accuracy of Large Datasets.

	TOG [2011]	TOG [2013]	TOG [2015]	Ours
Chair	80.20%	91.20%	92.52%	93.11%
Vase	69.90%	85.60%	88.54%	88.91%

ToG[2011] is short for Sidi et al. [TOG 2011], ToG[2013] is short for Kim et al.[TOG 2013],ToG[2015] is short for Guo et al.[2015].

testing in each experiment for each large dataset. In other words, the training sets gradually increase, while the test set remains the same, the results of which can be seen in Table 2. Because the work [Xie et al. 2014] carried similar experiment under 75% training condition with their method, we also make comparison with their results in Table 2. It can be seen from the table that the results obtained by our method performs better than theirs. Besides, with the increase of the training set, the classification accuracy of our method grows steadily in the same test set. This shows that with the increase of the training set, both the learning ability and the generalization ability of the network architecture become stronger, which also proves the effectiveness of the designed network in this paper.

Table 2: Labeling Accuracy of Large Datasets. Here are the results of the same test set for different number of training sets.

	Ours 25%	Ours 50%	Ours 75%	CGF[2014] 75%
Chair	93.43%	94.38%	95.91%	87.09%
Vase	88.04%	90.95%	91.17%	85.86%
Tele-alien	91.02%	92.76%	93.00%	83.23%

CGF[2014] is short for Xie et al.[CGF 2014]

Thirdly, we visualize the segmentation results obtained by using our method in the three large datasets of COSEG, as shown in Figure 9. All the results shown are optimized ones obtained using 75% training set. The segmentation results appear visually accurate, which proves the effectiveness of this method.

Mixed dataset training and testing are performed as well. We re-

spectively mix Airplane and Bird, Human and Teddy, which are of similar class. It must be noted that, unlike the method of [Guo et al. 2015] merging similar class labels, we retain these different labels, that is, body of the plane and bird are of different labels, their wings as well. 12 shapes of each dataset are selected as the training set, and the remaining as the test set. Our approach is repeated three times to compute the average performance, the segmentation results of which are shown in Figure 10. Figure 10(a) is part of the result of the training set while Figure 10(b) is part of the testing set. The classification accuracy of the two datasets is shown in Table 3, which suggests that we can get good segmentation results when mixing similar data together. Although the segmentation accuracy is not as high as training respectively, the average goes beyond 90%. Besides, the basic segmentation is correct by visualizing the results, which proves that the proposed network architecture is powerful in distinguishing features and learning.

Table 3: Labeling Accuracy of Mixed Datasets of Similar Shapes

	Aireplane & Bird	Human & Teddy
Accuracy	90.04%	92.28%

In addition, we mix Glasses and Plier, Glasses, Plier, Fish and Table of different categories. From the mixed datasets, we select some data for training, with the remaining for test. Here 12 shapes of each dataset are selected as the training set, and the remaining as the test set. We also mix two large datasets with 400 chairs and 300 vases, we selected 50% shapes for training from each dataset and the remaining 50% as the test set. Our approach is repeated three times to compute the average performance, the segmentation results of which are shown in Figure 11 and Figure 1. Figure 11(a) is part of the result of the training set while Figure 11(b) is part of the testing set. The classification accuracy of the three datasets is shown in Table 4, which indicates as well that both the segmentation results and classification accuracy achieve impressive performance. In other words, this method can be used to train and predict any shape set, and prove once again that our SFCN architecture has a good feature distinguishing ability and learning ability. Lastly, as in the papers of [Guo et al. 2015], we separately trained several small datasets of PSB when $N = 6$ and $N = 12$ (i.e., SB6, SB12), in which N is the number of randomly selected shapes in each training process. For each type of dataset, as in the papers

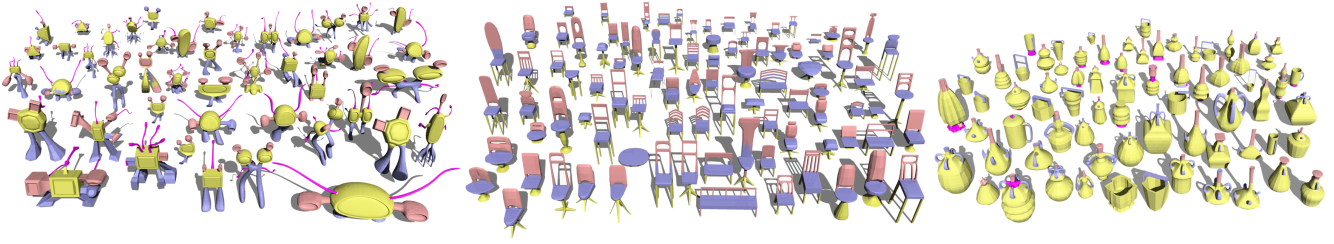


Figure 9: Results under Large Datasets

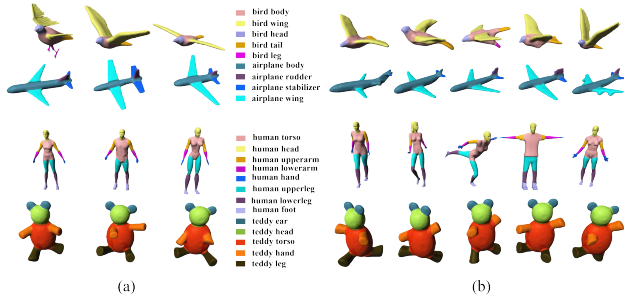


Figure 10: The Segmentation Results of Mixed Datasets of Similar Shapes. (a) Part of the shapes in the training set; (b) Segmentation results of part of the shape in the testing set.

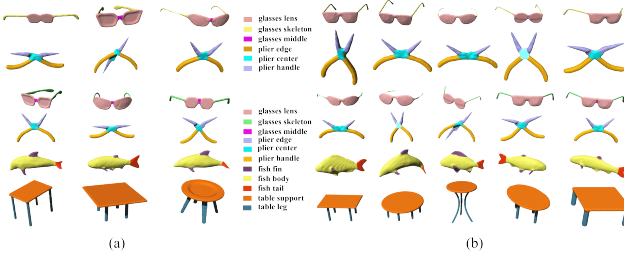


Figure 11: The Segmentation Results of Mixed Datasets of Different Shapes. (a) Part of the shapes in the training set; (b) Segmentation results of part of the shapeS in the testing set.

of [Guo et al. 2015], we repeat our approach five times to compute the average performance. The comparison results with the related methods are presented in Table 5. It should be noted that the results and data obtained by other methods comes from [Guo et al. 2015]. As shown in the Table 5, the results of several datasets of PSB obtained by our method do much better in most types than the existing methods [Kalogerakis et al. 2010; Guo et al. 2015; Xie et al. 2014; Wang et al. 2013; Chang and Lin 2007; Torralba et al. 2007], which has proven the effectiveness of the method. On a few individual datasets, such as Airplane, Chair and Table etc., our results does not go beyond that of other methods yet very close to the best ones, which can also prove our method is effective. Moreover, the segmentation effect gradually strengthens as the training data increases, which shows that the learning ability of the SFCN archi-

Table 4: Labeling Accuracy of Mixed Datasets of Different Shapes

	Glasses & Plier	Chair(400) & Vase(300)	Glasses & Plier & Fish & Table
Accuracy	96.53%	87.71%	91.82%

ture is enhanced with the increase of training samples. We also visualize segmentation results of several datasets of PSB including Teddy, Plier and Fish etc. on the condition of SB12, the optimized ones of which are shown in Figure 12. Just like the large dataset, the results of the small is visually accurate, which indicates the proposed method is feasible.

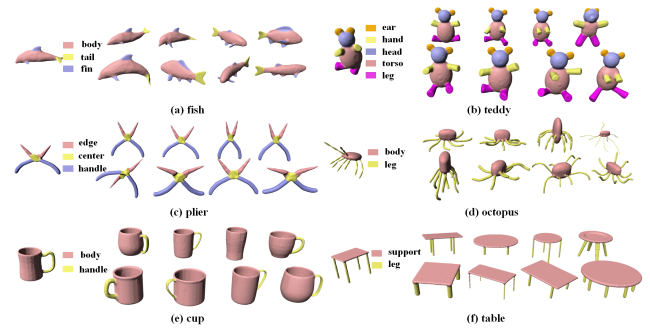


Figure 12: More results of our method.

Feature sensibility. In this paper, we combine three features, average geodesic distance (AGD) [Hilaga et al. 2001], shape context (SC) [Belongie et al. 2002] and spin image (SI) [Johnson and Hebert 1999] to complete the shape segmentation. To verify the validity of this combination, we carry out a comparative experiment. The classification accuracy of each dataset of PSB under a single feature and the one obtained with our method are compared in the condition of SB6, as shown in Figure 13. It can be seen that the classification accuracy of individual datasets under individual feature is higher but not too much than that of our method. On the contrary, most datasets perform much better by our method. It shows that the features selected in this paper are complementary and the feature combination is effective.

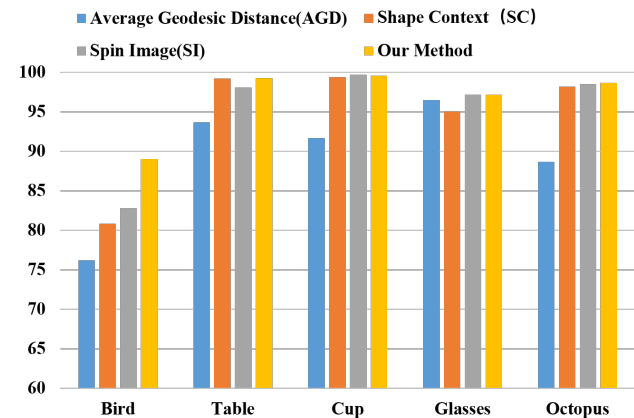


Figure 13: The Comparison of Segmentation Accuracy under Different Features

Table 5: Labeling Accuracy on Princeton Benchmark(SB6/SB12)

	SVM SB6	JointBoost SB6	ToG[2010] SB6	ToG[2013] SB6	ToG[2015] SB6	Ours SB6	ToG[2010] SB12	ToG[2013] SB12	ToG[2015] SB12	Ours SB12
Cup	94.11%	93.12%	99.1%	97.5%	99.49%	99.59%	99.60%	99.60%	99.73%	99.74%
Glasses	95.92%	93.59%	96.10%	-	96.78%	97.15%	97.20%	-	97.60%	97.79%
Airplane	80.43%	91.16%	95.50%	-	95.56%	93.90%	96.10%	-	96.67%	95.30%
Chair	81.38%	95.67%	97.80%	97.90%	97.93%	97.05%	98.40%	99.60%	98.67%	98.26%
Octopus	97.04%	96.26%	98.60%	-	98.61%	98.67%	98.40%	-	98.79%	98.80%
Table	90.16%	97.37%	99.10%	99.60%	99.11%	99.25%	99.30%	99.60%	99.55%	99.41%
Teddy	91.01%	85.68%	93.30%	-	98.00%	98.04%	98.10%	-	98.24%	98.27%
Plier	92.04%	81.55%	94.30%	-	95.01%	95.71%	96.20%	-	96.22%	96.55%
Fish	87.05%	90.76%	95.60%	-	96.22%	95.63%	95.60%	-	95.64%	95.76%
Bird	81.49%	81.80%	84.20%	-	87.51%	89.03%	87.90%	-	88.35%	89.48%
Mech	81.87%	75.73%	88.90%	90.20%	90.56%	91.72%	90.50%	91.30%	95.60%	96.05%
Average	88.41%	89.34%	94.77%	96.30%	95.89%	95.98%	96.12%	97.53%	96.82%	96.85%

ToG[2010] is short for Kalogerakis et al. [2010], ToG[2013] is short for Wang et al. [2013], ToG[2015] is short for Guo et al.[2015].

In the papers of [Kalogerakis et al. 2010] and [Guo et al. 2015], seven features are combined to do segmentation experiment. In addition to the three features used in this paper, they also use the other four features including curvature (CUR) [Kavukcuoglu et al. 2009], PCA feature (PCA) [Shapira et al. 2010], shape diameter function (SDF) [Liu et al. 2009] and distance from medial surface (DIS) [Long et al. 2015]. In this paper, several datasets of PSB are randomly selected to do experiment with the combination of seven features. In the same experiment condition, the comparison results with the combination of three features are presented in Figure 14. The experiment tells us that for most datasets, three features combination brings higher classification accuracy than seven features, and for the rest a few datasets, the classification accuracy of the two is very close to each other. This indicates that the three features used in this paper can not only better complement, but also more suitable for the network structure. In addition, the three features has the advantage of less computation, the SFCN parameters easy to adjust, and faster convergence of dataset, thus can quickly get good segmentation results.

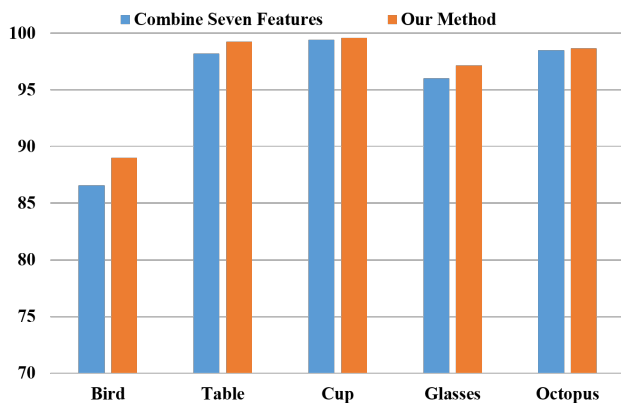


Figure 14: The Comparison between Segmentation Accuracy under Three Features and under Seven Features

Skip architecture. During the SFCN training process, we utilize skip architecture of five layers and integrate the cross layer information with different steps to improve the SFCN segmentation re-

sults, and gradually improve the segmentation details. To verify the skip architecture can do end-to-end learning and improve the segmentation results, we visualize the cross-layer prediction results with different steps. The segmentation results of several shapes crossing one to five layers are shown in Figure 15, where (f) is the groundtruth of the corresponding shape. Through the tracking of the network computing process, we found that the network convergence is faster with the increase of the cross layers. In addition, it can be seen from the comparison results of cross layers and groundtruth in Figure 15, with the increase of cross layers, the classification quality is gradually improved.

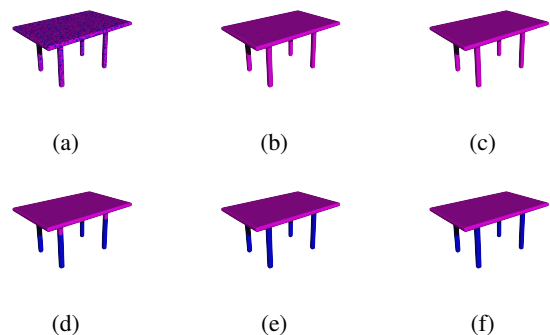


Figure 15: The Segmentation Results of Layer Information with Different Steps. (a)- (e) Segmentation results Crossing 1 to 5 layers; (f) Groundtruth.

Comparison before and after optimization. In this paper, we use multi-label graph cut optimization method [Boykov et al. 2001; Kolmogorov and Zabih 2004; Boykov and Kolmogorov 2004] to optimize the segmentation results of testing shape, based on the complementarity between features. The comparison results before and after optimization of several shapes are shown in Figure 16. As shown in Figure 16(a), the results before optimization are the final ones obtained by voting on the three different features tested by SFCN architecture. Figure 16(b) represents results after optimization. As the results before optimization is predicted in the triangle level, the boundary may be not smooth or there may be prediction errors of individual triangles in some areas. The above problems

are well addressed after the optimization with multi-label graph cuts optimization method [Boykov et al. 2001; Kolmogorov and Zabih 2004; Boykov and Kolmogorov 2004], which proves that the optimization plays a significant role. In addition, the number below each figure is the classification accuracy of the corresponding shape, which shows that the optimization can improve the classification accuracy.

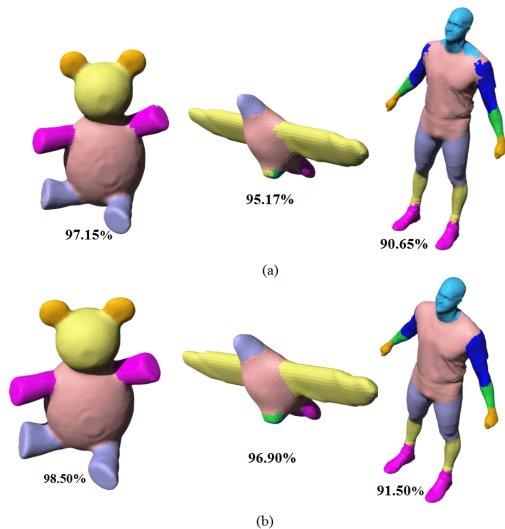


Figure 16: Comparison Results before and after optimization. (a) Segmentation results before optimization; (b) Segmentation results after optimization. The number below each shape is the segmentation accuracy of it.

Limitations. Although the proposed method can well complete the 3D shape segmentation task, it has some limitations. Firstly, the shapes involved in the calculation must be manifold meshes, for they can easily determine the connection between triangles. Secondly, the designed SFCN architecture has no feature selection function, thus we carry on the separate training for the three features. Besides, it is more reasonable that each feature should assign different weights to different types of shapes in the training process. Therefore, in the future work, we are going to improve the SFCN architecture, making it possible for automatic feature selection.

6 Conclusions

We propose a novel shape fully convolutional network architecture, which can automatically carry out end-to-end and triangles-to-triangles learning and prediction, and complete the segmentation task with high quality. In the SFCN architecture proposed here, similar to convolution and pooling operation on image, we first propose and implement shape convolution and pooling operation with the 3D shape represented as a graph structure. Moreover, based on the original image segmentation FCN architecture [Long et al. 2015], we first design and implement new generating operation, which functions as a bridge to facilitate the execution of shape convolution and pooling operation directly on 3D shape. Besides, accurate and detailed segmentation of the 3D shapes is completed through skip architecture. To produce more accurate segmentation results, we optimize the segmentation results obtained by SFCN prediction by utilizing the complementarity between the three geometric features and the multi-label graph cut method [Boykov et al. 2001; Kolmogorov and Zabih 2004; Boykov and Kolmogorov 2004], which can also improve the local smoothness of triangle labels. The experiments show that the

proposed method can not only obtain good segmentation results both in large datasets and small ones with the use of a small number of features, but also outperform some existing state-of-the-art shape segmentation methods. More importantly, our method can effectively learn and predict mixed shape datasets either of similar or of different characters, and achieve excellent segmentation results, which demonstrate our method has strong generalization ability.

In the future, we want to strengthen our method to overcome some limitations mentioned above, such as, selecting features automatically. Besides, we hope the SFCN architecture proposed can be applied to other shape fields, such as shape synthesis, line drawing extraction and so on.

References

- BELONGIE, S., MALIK, J., AND PUZICHA, J. 2002. Shape matching and object recognition using shape contexts. *IEEE Transactions on Pattern Analysis & Machine Intelligence* 24, 4, 509–522.
- BOYKOV, Y., AND KOLMOGOROV, V. 2004. An experimental comparison of min-cut/max-flow algorithms for energy minimization in vision. *IEEE Transactions on Pattern Analysis & Machine Intelligence* 26, 9, 1124–37.
- BOYKOV, Y., VEKSLER, O., AND ZABIH, R. 2001. Efficient approximate energy minimization via graph cuts. *IEEE Transactions on Pattern Analysis & Machine Intelligence* 20, 12, 1222–1239.
- CHANG, C.-C., AND LIN, C.-J. 2007. Libsvm: A library for support vector machines. *Acm Transactions on Intelligent Systems & Technology* 2, 3, article 27, 389–396.
- CHEN, X., LEKSEY GOLOVINSKIY, AND FUNKHOUSER, T. 2009. A benchmark for 3d mesh segmentation. *Acm Transactions on Graphics* 28, 3, 341–352.
- CHEN, X., ZHOU, B., LU, F., TAN, P., BI, L., AND TAN, P. 2015. Garment modeling with a depth camera. *ACM Transactions on Graphics* 34, 6, 1–12.
- CIRESAN, D., GIUSTI, A., GAMBARDELLA, L. M., AND SCHMIDHUBER, J. 2012. Deep neural networks segment neuronal membranes in electron microscopy images. In *Advances in neural information processing systems*, 2843–2851.
- DEFFERRARD, M., BRESSON, X., AND VANDERGHEYNST, P. 2016. Convolutional neural networks on graphs with fast localized spectral filtering.
- DHILLON, I. S., GUAN, Y., AND KULIS, B. 2007. Weighted graph cuts without eigenvectors: A multilevel approach. In *IEEE Trans. Pattern Anal. Mach. Intell.*, 2007.
- DOSOVITSKIY, A., FISCHER, P., ILG, E., H’AUSSER, P., HAZRBA, C., GOLKOV, V., VAN DER SMAGT, P., CREMERS, D., AND BROX, T. 2015. Flownet: Learning optical flow with convolutional networks. 2758–2766.
- EDWARDS, M., AND XIE, X. 2016. Graph based convolutional neural network.
- FARABET, C., COUPRIE, C., NAJMAN, L., AND LECUN, Y. 2013. Learning hierarchical features for scene labeling. *IEEE Transactions on Pattern Analysis & Machine Intelligence* 35, 8,

- 1915–29.
- GAL, R., AND COHEN-OR, D. 2006. Salient geometric features for partial shape matching and similarity. *Acm Transactions on Graphics* 25, 1, 130–150.
- GUO, K., ZOU, D., AND CHEN, X. 2015. 3d mesh labeling via deep convolutional neural networks. *ACM Transactions on Graphics* 35, 1 (Dec.), 3.
- HILAGA, M., SHINAGAWA, Y., KOHMURA, T., AND KUNII, T. L. 2001. Topology matching for fully automatic similarity estimation of 3d shapes. In *Conference on Computer Graphics and Interactive Techniques*, 203–212.
- HU, R., FAN, L., AND LIU, L. 2012. Co-segmentation of 3d shapes via subspace clustering. *Computer Graphics Forum* 31, 5, 17031713.
- HUANG, Q., KOLTUN, V., AND GUIBAS, L. 2011. Joint shape segmentation with linear programming. 61–64.
- JIA, Y., SHELHAMER, E., DONAHUE, J., KARAYEV, S., LONG, J., GIRSHICK, R., GUADARRAMA, S., AND DARRELL, T. 2014. Caffe: Convolutional architecture for fast feature embedding. *Eprint Arxiv*, 675–678.
- JOHNSON, A. E., AND HEBERT, M. 1999. Using spin images for efficient object recognition in cluttered 3d scenes. *IEEE Transactions on Pattern Analysis & Machine Intelligence* 21, 5, 433–449.
- KALOGERAKIS, E., HERTZMANN, A., AND SINGH, K. 2010. Learning 3d mesh segmentation and labeling. *Acm Transactions on Graphics* 29, 4, 157–166.
- KAVUKCUOGLU, K., RANZATO, M., FERGUS, R., AND LECUN, Y. 2009. Learning invariant features through topographic filter maps. In *IEEE Conference on Computer Vision & Pattern Recognition*, 1605–1612.
- KIM, V. G., LI, W., MITRA, N. J., CHAUDHURI, S., DIVERDI, S., AND FUNKHOUSER, T. 2013. Learning part-based templates from large collections of 3d shapes. *Acm Transactions on Graphics* 32, 4, 1.
- KOLMOGOROV, V., AND ZABIH, R. 2004. What energy functions can be minimized via graph cuts? *Pattern Analysis & Machine Intelligence IEEE Transactions on* 26, 2, 147–59.
- KREAVOY, V., JULIUS, D., AND SHEFFER, A. 2007. Model composition from interchangeable components. In *Conference on Computer Graphics & Applications*, 129–138.
- KRIZHEVSKY, A., SUTSKEVER, I., AND HINTON, G. E. 2012. Imagenet classification with deep convolutional neural networks. *Advances in Neural Information Processing Systems* 25, 2, 2012.
- LIU, R., ZHANG, H., SHAMIR, A., AND COHEN-OR, D. 2009. A part-aware surface metric for shape analysis. *Computer Graphics Forum* 28, 2, 397406.
- LIU, F., SHEN, C., LIN, G., AND REID, I. 2015. Learning depth from single monocular images using deep convolutional neural fields. *IEEE Transactions on Pattern Analysis & Machine Intelligence* 38, 10, 1–1.
- LONG, J., SHELHAMER, E., AND DARRELL, T. 2015. Fully convolutional networks for semantic segmentation. In *Computer Vision and Pattern Recognition*, 3431–3440.
- MENG, M., XIA, J., LUO, J., AND HE, Y. 2013. Unsupervised co-segmentation for 3d shapes using iterative multi-label optimization. *Computer-Aided Design* 45, 2, 312–320.
- NIEPERT, M., AHMED, M., AND KUTZKOV, K. 2016. Learning convolutional neural networks for graphs.
- PINHEIRO, P. H. O., AND COLLOBERT, R. 2013. Recurrent convolutional neural networks for scene parsing. 82–90.
- SHAPIRA, L., SHALOM, S., SHAMIR, A., COHEN-OR, D., AND ZHANG, H. 2010. Contextual part analogies in 3d objects. *International Journal of Computer Vision* 89, 2, 309–326.
- SIDI, O., VAN KAICK, O., KLEIMAN, Y., ZHANG, H., AND COHEN-OR, D. 2011. Unsupervised co-segmentation of a set of shapes via descriptor-space spectral clustering. In *SIG-GRAPH Asia Conference*, 1.
- SIMO-SERRA, E., IIZUKA, S., SASAKI, K., AND ISHIKAWA, H. 2016. Learning to simplify: Fully convolutional networks for rough sketch cleanup. *Acm Transactions on Graphics* 35, 4, 1–11.
- SIMONYAN, K., AND ZISSERMAN, A. 2014. Very deep convolutional networks for large-scale image recognition. *Computer Science*.
- SZEGEDY, C., LIU, W., JIA, Y., SERMANET, P., REED, S., ANGUELOV, D., ERHAN, D., VANHOUCHE, V., AND RABINOVICH, A. 2015. Going deeper with convolutions. 1–9.
- TORRALBA, A., MURPHY, K. P., AND FREEMAN, W. T. 2007. Sharing visual features for multiclass and multiview object detection. *IEEE Transactions on Pattern Analysis & Machine Intelligence* 29, 5, 854–869.
- WANG, Y., ASAFIY, S., VAN KAICK, O., ZHANG, H., COHEN-OR, D., AND CHEN, B. 2012. Active co-analysis of a set of shapes. *Acm Transactions on Graphics* 31, 6, 157:1–157:10.
- WANG, Y., GONGY, M., WANG, T., COHEN-OR, D., ZHANG, H., AND CHEN, B. 2013. Projective analysis for 3d shape segmentation. *Acm Transactions on Graphics* 32, 6, 1–12.
- XIE, S., AND TU, Z. 2015. Holistically-nested edge detection. In *IEEE International Conference on Computer Vision*, 1395–1403.
- XIE, Z., XU, K., LIU, L., AND XIONG, Y. 2014. 3d shape segmentation and labeling via extreme learning machine. *Computer Graphics Forum* 33, 5, 85–95.
- XU, K., LI, H., ZHANG, H., COHEN-OR, D., XIONG, Y., AND CHENG, Z.-Q. 2010. Style-content separation by anisotropic part scales. *Acm Transactions on Graphics* 29, 6, 184.
- YANG, Y., XU, W., GUO, X., ZHOU, K., AND GUO, B. 2013. Boundary-aware multi-domain subspace deformation. *IEEE Transactions on Visualization & Computer Graphics* 19, 19, 1633–45.
- YU, Y., ZHOU, K., XU, D., SHI, X., BAO, H., GUO, B., AND YEUNG, S.-H. 2004. Mesh editing with poisson-based gradient field manipulation. *ACM Transactions on Graphics* 23, 3, 644–651.